Published online 11 December 2020

Nucleic Acids Research, 2021, Vol. 49, No. 1 ***383–399***
doi: 10.1093/nar/gkaa1180

Ribosome profiling reveals ribosome stalling on tryptophan codons and ribosome queuing upon oxidative stress in fission yeast

Angela Rubio[1], Sanjay Ghosh[1], Michael Mülleder[2], Markus Ralser[2,3] and Juan Mata[1,*]

[1]Department of Biochemistry, University of Cambridge, UK, [2]The Molecular Biology of Metabolism Laboratory, The Francis Crick Institute, London, UK and [3]Department of Biochemistry, Charité University Medicine, Berlin, Germany

Received May 05, 2020; Revised November 13, 2020; Editorial Decision November 17, 2020; Accepted November 19, 2020

ABSTRACT

Translational control is essential in response to stress. We investigated the translational programmes launched by the fission yeast *Schizosaccharomyces pombe* upon five environmental stresses. We also explored the contribution of defence pathways to these programmes: The Integrated Stress Response (ISR), which regulates translation initiation, and the stress-response MAPK pathway. We performed ribosome profiling of cells subjected to each stress, in wild type cells and in cells with the defence pathways inactivated. The transcription factor Fil1, a functional homologue of the yeast Gcn4 and the mammalian Atf4 proteins, was translationally upregulated and required for the response to most stresses. Moreover, many mRNAs encoding proteins required for ribosome biogenesis were translationally downregulated. Thus, several stresses trigger a universal translational response, including reduced ribosome production and a Fil1-mediated transcriptional programme. Surprisingly, ribosomes stalled on tryptophan codons upon oxidative stress, likely due to a decrease in charged tRNA-Tryptophan. Stalling caused ribosome accumulation upstream of tryptophan codons (ribosome queuing/collisions), demonstrating that stalled ribosomes affect translation elongation by other ribosomes. Consistently, tryptophan codon stalling led to reduced translation elongation and contributed to the ISR-mediated inhibition of initiation. We show that different stresses elicit common and specific translational responses, revealing a novel role in Tryptophan-tRNA availability.

INTRODUCTION

Cells react to stress situations such as starvation, changes in temperature, or the presence of toxic substances in their environment, by transcriptome and translation remodelling, as well as by the reconfiguration of their metabolism. Translation is the most energy-consuming process of the cell. Therefore, translational control plays an essential role by determining the rate of protein synthesis, which helps shape the composition of the proteome. Compared to transcriptional regulation, translational control of existing mRNAs allows for more rapid changes in protein levels, making this process particularly important upon stress exposure (1). In addition, as protein synthesis requires a large proportion of the cell energy, its regulation is related to the metabolic status of the cell (2). Therefore, a tight control of translation is essential to cope with stress situations, and misregulation of this process often leads to disease (3).

In eukaryotes, translational control is often performed at the initiation stage (4), when the AUG start codon is identified and decoded by the initiator tRNA (Met-tRNAi Met). A key regulator of this process is the translation initiation factor eIF2, which is part of the so-called ternary complex (TC) together with the initiator tRNA and GTP. The TC, in complex with other translation initiation factors, binds to the 40S ribosomal subunit to form the 43S preinitiation complex (PIC). The 43S PIC is recruited to the 5′ cap of the mRNA by additional initiation factors, leading to the formation of the 48S PIC, which scans the mRNA until the initiation codon is reached. At this step, the 60S subunit binds the complex and GTP is hydrolysed. eIF2-GDP must then be recycled to eIF2-GTP by the GTP/GDP-exchange factor eIF2B. After stress exposure, the eIF2α subunit is phosphorylated at a specific serine residue (serine 51 in mammals and 52 in fission yeast), and binds to eIF2B acting as a competitive inhibitor, which reduces levels of the ternary complex and triggers a global down-regulation of translation (5,6).

*To whom correspondence should be addressed. Tel: +44 1223760467; Email: jm593@cam.ac.uk
Present address: Sanjay Ghosh, Institute of Bioinformatics and Applied Biotechnology, Bengaluru, India.

The pathway that regulates translation through eIF2α phosphorylation is called the Integrated Stress Response. In mammals, there are four eIF2α kinases (Hri, Gcn2, Pek/Perk and Pkr) that are activated by different stresses and inhibit translation initiation through the phosphorylation of eIF2α (4). In the yeast *Saccharomyces cerevisiae*, Gcn2 is the sole eIF2α kinase (7,8). In the fission yeast *Schizosaccharomyces pombe*, three eIF2α kinases (Gcn2, Hri1 and Hri2) show distinct and overlapping activation patterns in response to cellular stresses (9,10). Whereas Hri2 is mainly activated in response to heat shock and Hri1 at stationary phase in response to nutritional limitation, Gcn2 is the main eIF2α kinase activated in early exposure to H_2O_2 and MMS (9–11).

In parallel to the general downregulation of translation upon stress, there is an induction of the translation of specific mRNAs, some of them encoding transcription factors, which in turn promote the transcriptional response. Recently, we have shown that amino acid starvation in *S. pombe* increases the translation of the transcription factor Fil1, the functional orthologue of Atf4 in mammals and Gcn4 in budding yeast, through the activation of the Gcn2–eIF2α pathway (12). Fil1 is required for the transcriptional response to amino acid starvation as well as for normal growth in minimal medium lacking amino acids. Furthermore, Fil1 is regulated in a similar manner through inhibitory upstream ORFs (uORFs) located at the 5′-leader sequence (six uORFs in *fil1*, four in *GCN4* and two in *ATF4*) (12). In budding yeast and mammalian cells, eIF2α phosphorylation reduces the abundance of active ternary complexes and the reinitiation of translation occurs after bypassing the inhibitory uORFs, which allows the scanning subunit to reach the main coding sequence (8,13). Notably, Fil1 does not show sequence similarity to either Gcn4 or Atf4 (12).

Gene expression programs in response to stress are also regulated by Stress Activated Protein Kinases (SAPK). A key player in this pathway in *S. pombe* is the mitogen-activated protein kinase (MAPK) Sty1/Spc1 (14,15), which is homologous to the Hog1 osmo-sensing MAPK in *S. cerevisiae* and to the mammalian and *Drosophila* JNK and p38 SAPKs (16).

Stress signals activate and phosphorylate Sty1, promoting its transient accumulation in the nucleus, where it triggers a wide transcriptional shift of the gene expression program. This transcriptional response is mediated by the Atf1 transcription factor (17–20). Sty1 also has a role in the translational response to stress. First, cells show higher levels of eIF2α phosphorylation in the absence of Sty1 (10,21). Second, Sty1 associates *in vivo* with the translation elongation factor 2 (eEF2) and the translation initiation factor 3a (eIF3a) (22). Finally, the presence of Sty1 is required to maintain the levels and the phosphorylation of eIF3a, and the recovery of translation levels after stress is less efficient in the absence of Sty1 (21,22).

Translation upon stress can be also regulated at the elongation step through the abundance, modification, and charging levels of transfer RNA (tRNA) (23). tRNA is the most extensively modified RNA and many post-transcriptional nucleoside modifications occur at the anticodon loop (24). These modifications can change the stability or localization of tRNAs (25), as well as the fidelity and efficiency of translation (26). It has also been shown that tRNA fragmentation appears upon stress in eukaryotes (27) and, in human cells, that tRNA fragments have a role in translation repression (28).

Ribosome profiling (ribo-seq) provides a genome-wide and high-resolution view of translational control. The approach is based on the treatment of translating ribosome–mRNA complexes with a ribonuclease (RNase), in such a way that only RNA fragments protected by bound ribosome survive the treatment. These fragments are then isolated and analysed by high-throughput sequencing. The number of sequence reads that map to a coding sequence, normalized by mRNA levels, provides an estimate of the efficiency of translation for every cellular mRNA (29). In addition, the position of the reads on the genome identifies the location of ribosomes on the mRNA. This information can be used to determine relative ribosome occupancies on each codon, which allow the detection of ribosomes stalled on specific codons (12,30,31).

Although some stress-induced gene expression programs have been studied in detail at the genome-wide level (14,15,32–36), the effects of different stresses have been examined in isolation, making comparisons across stresses difficult. Moreover, to our knowledge, there are no systematic studies of the role of major stress-response pathways on genome-wide translation programmes. Here we use *S. pombe* to investigate similarities and differences among the translational responses to five commonly studied stress situations: exposure to H_2O_2 (oxidative stress), cadmium (heavy metal), and methyl methanesulfonate (MMS, genotoxic stress), sorbitol treatment to induce osmotic shock, and heat shock. We perform ribosome profiling in control and stressed cells, under highly controlled conditions. We also investigate the contribution of the Integrated Stress Response (mediated by eIF2α phosphorylation) and the stress-responsive MAPK pathway (Sty1) to these translation programs. Overall, we found that translation is typically downregulated, but activated for very few genes. Interestingly, the Fil1 transcription factor is highly induced at the translational level upon several stresses, in a manner dependent on eIF2α phosphorylation. Moreover, Fil1 is required for the full implementation of stress-responsive transcription programs. These stresses also cause a rapid translational downregulation of genes involved in ribosome biogenesis and ribosomal proteins.

Surprisingly, we found that ribosomes stall selectively on tryptophan codons upon oxidative stress, a phenomenon that is likely to be caused by a decrease in the levels of charged tRNA-Tryptophan (tRNA-Trp). This specific stalling on tryptophan codons led to an elongation defect and to ribosome collisions / queuing upstream of stalled ribosomes. Our results suggest that different stresses elicit common and specific translational responses, both at the initiation and the elongation levels, and uncovers a novel and specific role to tryptophan tRNA availability.

MATERIALS AND METHODS

Strains, growth conditions and experimental design

All strains used were prototrophic. Supplementary Table S1 presents a full list of strains. Standard methods and media were used for *S. pombe* (37). For all genome-wide stress

experiments, *S. pombe* cells were grown in YES medium (supplemented with leucine, uracil and adenine) at 32°C. Cells were treated for 15 min as described below. Heavy metal stress: cadmium sulphate ($CdSO_4$; 481882; Sigma) was added to a final concentration of 0.5 mM. Oxidative stress: hydrogen peroxide (H_2O_2; H1009; Sigma) was added to a final concentration 0.5 mM. Heat stress: cells were quickly transferred from 32°C to a prewarmed flask in a 39°C water bath. Alkylating agent: methyl methanesulfonate (MMS, 129925, Sigma) at a final concentration of 0.02%. Osmotic stress: cells were grown to $OD_{600} = 0.7$, and diluted with prewarmed YES 3 M sorbitol (BP-439–500, Fisher) to a final concentration 1 M sorbitol. A control unstressed culture was processed in parallel for each of the stresses (a total of 10 control samples for each genetic background).

For plate drop assays, cells were grown in YES to exponential phase at 32°C and plated in 10-fold dilutions. Plates were incubated for two days at 32°C (except the plate incubated at 39°C for heat shock assays). For tryptophan charging experiments, supplemental tryptophan (DOC0188, Formedium) was added to the culture from a stock 8 g/l in YES to a final concentration of 200 mg/l.

All repeats of genome-wide experiments were independent biological replicates carried out on separate days (see ArrayExpress deposition footnote for a complete list). The following sequencing experiments were performed: (i) ribosome profiling and matching RNA-seq in five stress conditions of three strains (wild-type, *eIF2α-S52A* and *sty1Δ*) and (ii) RNA-seq of *fil1Δ* and cells in five stress conditions.

Amino acid analysis

Amino acid quantification was performed by liquid chromatography selective reaction monitoring (LC-SRM) as described (38).

Protein analyses

To prepare samples for Western blotting, cells were harvested by filtration, washed with 20% TCA, resuspended in 100 μl of 20% TCA, and frozen. Cell pellets were lysed with 1 ml of acid-treated glass beads in a bead beater (FastPrep-5; MP Biomedicals) at level 7.5 for 15 s, and 400 μl of 5% TCA was added before eluting from the glass beads. Lysates were frozen on dry ice and spun at 18 000 relative centrifugal force for 10 min. Pellets were resuspended in SDS-Tris solution (2% SDS and Tris 0.3M pH 10.7), boiled during 5 min and cleared by centrifugation at maximum speed for 2 min. Protein extract concentrations were measured using Pierce BCA Protein Assay solution (Thermo), and 60–90 μg of total protein were loaded with Laemmli SDS Sample Buffer (reducing) (Alfa Aesar). For western blot analysis, the following antibodies were used: anti-eIF2α (1:500; 9722, Cell Signalling), anti-Phospho-eIF2α (1:1,000; 9721, Cell Signalling), and anti-tubulin (1:10 000; sc-23948, Santa Cruz). The secondary antibodies were HRP-conjugated goat anti-mouse IgG (H+L) (1:10 000; 31430, Thermo Fisher) and anti-rabbit IgG (1:10 000; ab-6721, Abcam). TAP tag was detected with peroxide–anti-peroxide complexes (P1291; Sigma). Detection was performed using the enhanced chemiluminescence procedure (ECL kit).

Northern analysis of aminoacyl-tRNA charging

RNA from the indicated conditions was prepared by phenol extraction under acidic conditions using acid buffer (0.3 M sodium acetate pH 5, 10 mM Na_2EDTA) for resuspension of frozen cells, and final acid RNA buffer (10 mM sodium acetate pH 5, 1 mM EDTA). As control samples, RNA was deacylated with 0.2 M Tris pH 9.0 for 2h at 37°C. Periodate oxidation and β-elimination were performed as described (39) using 2 μg of total RNA. In the final step, all samples were deacylated. tRNAs were detected by northern blotting in non-acidic conditions: RNA samples were loaded onto a 6.5% denaturing urea polyacrylamide gel, electrophoresed at 17 W for 70 min and transferred onto an Amersham Hybond-N membrane (GE Healthcare) using the Transblot SD semi-dry transfer cell (Biorad) as described (40), but using non-acidic conditions. The oligonucleotide probes used were: tRNA Trp CCA (5′-TGACCCCTAAGTGACT TGAACACTTGA-3′), tRNA His GUG (5′- TGCCCACA CCAGGAATCGAACCTGGGT-3′) and U5 snRNA as loading control (5′- GCACACCTTACAAACGGCTGTT TCTG-3′) (39). The oligonucleotides were labelled with infrared dyes (IRD-700 or IRD-800) at the 5′ end for fluorescence detection using the LICOR Odyssey system. The tRNA loading was quantified as the ratio of upper to lower bands relative to the unstressed condition. Significance was calculated using a two-sided paired Student's *t*-test.

Polysome profiling, ribosome profiling, library preparation and sequencing

Ribosome-protected fragment (RPF) analyses, preparation of cell extracts, RNase treatment, separation of samples by centrifugation through sucrose gradients, and isolation of protected RNA fragments were performed as described (41). Note that cycloheximide was not added to the culture before collection, and that cells were collected by filtration followed by flash-freezing. For polysome profiles, there is no RNase I digestion step, and lysis buffer and sucrose solutions were prepared with double concentration of $MgCl_2$ (10 mM). Polysome-subpolysome ratio was quantified by measuring the area under the curve using Image J software (NIH).

For all RPF samples, gel-purified RNA fragments of around 17–30 nucleotides were treated with 10 units of T4 PNK (Thermo Fisher) in a low-pH buffer (700 mM Tris, pH 7, 50 mM DTT and 100 mM $MgCl_2$) for 30 min at 37°C. ATP and buffer A (Thermo Fisher) were then added for an additional 30 min incubation. RNA fragments were column-purified (PureLink RNA microcolumns; Life Technologies). A total of 100 ng was used as input for the NEXTFLEX Small RNA Sequencing Kit (Version 3; Bioo Scientific), and libraries were generated following the manufacturer's protocol. For mRNA analyses, total RNA was isolated as described (41). Total RNA was then depleted from rRNA by using Ribo-Zero Gold rRNA Removal Kit Yeast (Illumina) with 4 μg as input. Finally, 30 ng of rRNA-depleted RNA was used as starting material for

the NEXTflex Rapid Directional qRNA-Seq Kit (Bioo Scientific). Libraries were sequenced in an Illumina HiSeq4000 or Novaseq6000 as indicated (ArrayExpress submission).

Data analysis

Data processing and read alignment were performed as described (12). Data quantification (number of reads per coding sequence) was carried out by using in-house Perl scripts as described (12). All statistical analyses were performed using R. Raw counts for mRNAs and RPFs are presented in Supplementary Datasets S1 and S2.

Differential expression analysis was performed by using the Bioconductor DESeq2 package (42). Raw counts were directly fed to the program, and no filtering was applied. Unless otherwise indicated, a threshold of 10^{-2} was chosen for the adjusted *P* value, and a cut-off of 2-fold minimal change in RNA levels.

For codon usage analysis, only codons after 90 were used. For each coding sequence, the following calculations were performed: (i) determination of the fraction of RPFs that occupy each codon (RPFs in a given codon divided by total RPFs); (ii) quantification of the relative abundance of each codon on the coding sequence (number of times each codon is present divided by total codon number); and (iii) definition of the normalized codon occupancy by dividing parameter 1 by parameter 2. The average codon enrichments) were then calculated with data from all coding sequences. The codon occupancies represented correspond to the A-site position.

For relative translational efficiencies analysis we used RiboDiff (43). RiboDiff was provided with raw read counts for each gene, from ribosome profiling and from RNA-seq. To select differentially translated genes, a threshold of 10^{-2} for the adjusted *P* value, and a cut-off of 1.5-fold were chosen.

Translation efficiency and mRNA ratios were median-centred for plotting. The list of Fil1 targets for Figure 4 and Supplementary Figure S3 was obtained from reference (12) as follows: Dataset_S01, repressed genes in *fil1Δ versus* wild type without stress (no 3AT) and only those genes from the lists with at least 20 counts in 80% or more samples were used. Gene set enrichment was performed with AnGeLi (44). The significance of the overlap between gene lists was calculated using Fisher's exact test.

RESULTS

Transcriptomic responses to stress

To investigate genome-wide effects of stress on gene expression, we carried out two independent ribosome profiling experiments (with parallel RNA-seq) of *S. pombe* cells subjected to five different stress-inducing treatments for 15 min: 0.5 mM H_2O_2 (oxidative stress, can also cause DNA damage), 0.5 mM $CdSO_4$ (heavy metal exposure), temperature shift from 32 to 39°C (heat shock), 1 M sorbitol (osmotic shock) and 0.02% methyl methanesulfonate (MMS, an alkylating agent that causes DNA damage). To study the contribution of the eIF2α phosphorylation and Sty1 pathways we performed parallel experiments with the mutant strain *eIF2α-S52A*, which expresses a non-phosphorylatable version of eIF2α, and a *sty1Δ* strain, in which the main stress-responsive MAPK pathway is inactive. These conditions have been used in the past for microarray-based transcriptomics, and have been shown to elicit robust transcriptional responses within a similar timeframe while maintaining high cell viability (14). All experiments were carried out using rich medium (YE), as *sty1Δ* cells grow very poorly in minimal medium.

We first examined the transcriptional responses to stress using the RNA-seq data (Supplementary Dataset S1). As we did not perform a global correction for total mRNA abundance, the discussion below refers to relative changes in gene expression. Supplementary Figure S1A shows a heat map with over 1200 genes that are differentially expressed in at least one condition in wild-type cells. There were more genes significantly up-regulated than down-regulated in every strain and condition (Table 1). Under the specific stress conditions that we employed (i.e. concentration of stressor and time), the changes were more extensive after heat and cadmium treatments, but genes induced by the five stress treatments overlapped significantly with one another. A similar overlap across stresses was observed for repressed genes (highest *P* value $< 2 \times 10^{-5}$ in wild type cells) (Supplementary Dataset S3).

Most of the regulated genes behaved similarly in wild type and *eIF2α-S52A* cells, and the induced and repressed transcripts lists overlapped significantly between both strains (Supplementary Figure S1A). However, fewer transcripts in *eIF2α-S52A* cells than in wild type reached the significance threshold (Table 1). Direct comparisons between *eIF2α-S52A* and wild type cells under stress (Table 2) (Supplementary Dataset S4) revealed that genes that were expressed at lower levels in the mutant were enriched in GO categories such as DNA integration (GO:0015074, $P = 10^{-12}$), anion transport (GO:0006820, $P = 10^{-4}$) and transmembrane transport (GO:0055085, $P = 10^{-4}$). There were also changes in the expression of the targets of the Fil1 transcription factor, which are discussed in detail below.

By contrast, the transcriptional response to stress in *sty1Δ* cells was substantially weaker although not completely abolished (14) (Supplementary Figure S1A). Consistently, the numbers of induced and repressed genes were much lower in *sty1Δ* cells (Table 1). Transcripts expressed at higher levels in *sty1Δ* mutants with respect to wild type cells (Table 2, Supplementary Dataset S4,) included genes involved in ribosome biogenesis (GO:0042254; $P = 10^{-30}$) and ncRNA processing (GO:0034470; $P = 10^{-14}$). Both categories are strongly enriched in transcripts that are repressed in wild type cells upon stress treatments (Supplementary Dataset S3) ($P = 10^{-50}$ and $P = 10^{-49}$), indicating that Sty1 is required for their normal repression in response to stress.

We also identified dozens of differentially expressed non-protein coding RNAs after stress treatments (Table 3, Supplementary Dataset S5), many of them predicted to be antisense to coding transcripts. Interestingly, we found that the non-coding *meiRNA*, which is involved in switching from mitotic to meiotic cell cycle (45,46), was induced after heat shock and sorbitol treatments.

Table 1. Number of differentially expressed transcripts after stress exposure on each strain. Numbers of mRNAs regulated in the five stress conditions in three genetic backgrounds: wild type, *eIF2α-S52A* and *sty1Δ* cells. mRNA up/down, and translation up/down indicate numbers of mRNAs whose expression is significantly up- or down-regulated at the transcriptome or translational levels, respectively (see Methods for details). Annotated lists containing these genes are presented in Supplementary Dataset S3

	mRNA up			mRNA down			Translation up			Translation down		
	wt	*S52A*	*sty1Δ*	*wt*	*S52A*	*sty1Δ*	*wt*	*S52A*	*sty1Δ*	*wt*	*S52A*	*sty1Δ*
$CdSO_4$	443	410	176	302	269	111	57	37	17	320	212	103
HS	621	468	306	404	364	149	39	18	1	229	124	5
H_2O_2	186	120	25	36	50	18	7	1	3	49	0	65
MMS	142	147	0	8	22	0	4	2	0	1	0	0
Sorbitol	193	198	0	113	109	0	0	0	0	1	1	7

Table 2. Number of differentially expressed transcripts on mutant strains relative to wild type. Numbers of mRNAs whose expression is differentially regulated in no stress and five stress conditions in the mutants *eIF2α-S52A* and *sty1Δ* cells relative to wild type cells. Annotated lists containing these genes are presented in Supplementary Dataset S4

	mRNA up		mRNA down	
	S52A	*sty1Δ*	*S52A*	*sty1Δ*
No stress	60	72	6	133
$CdSO_4$	37	199	13	325
HS	101	409	116	469
H_2O_2	136	171	82	360
MMS	54	121	15	303
Sorbitol	29	105	10	353

Table 3. Number of differentially expressed non-coding transcripts after stress exposure for each strain. Numbers of ncRNAs whose expression is differentially regulated in the five stress conditions in three genetic backgrounds: wild type, *eIF2α-S52A* and *sty1Δ* cells. Annotated lists containing these genes are presented in Supplementary Dataset S5

	mRNA up			mRNA down		
	wt	*S52A*	*sty1Δ*	*wt*	*S52A*	*sty1Δ*
$CdSO_4$	151	176	100	43	33	1
HS	216	169	121	70	21	8
H_2O_2	6	2	4	0	0	0
MMS	11	21	1	2	3	0
Sorbitol	45	32	2	8	11	0

The Core Environmental Stress Response (CESR) was defined in a microarray study as those genes induced or repressed two-fold or greater in most of the five stresses analysed (14). Consistent with the microarray data, the majority of induced and repressed CESR genes, as well as stress-specific genes, were also differentially expressed in our RNA-seq experiments (Figure 1A, B and Supplementary Figure S1B, C). The expression of Fil1 targets in *sty1Δ* cells is discussed below. Overall, our data show that transcriptomic responses to stress are largely independent of eIF2α phosphorylation, but reliant on the MAPK pathway

General translational responses to stress

Activation of the Integrated Stress Response by stress leads to general translational down-regulation, mediated through eIF2α phosphorylation. To investigate the level of activation of this pathway and its effect on global translation levels, we monitored eIF2α phosphorylation levels by immunoblotting and analysed polysome profiles using sucrose gradients. For the specific conditions we used (see above), cadmium, heat shock and H_2O_2 treatments led to increased eIF2α phosphorylation levels (Figure 1C) and lower polysomes to subpolysomes ratios (Figure 1D-G, Supplementary Figure S2A, B), the latter being indicative of a decrease in translation initiation. By contrast, both effects were not observed after MMS and sorbitol treatments (Figure 1C, G, Supplementary Figure S2A, B). *eIF2α-S52A* cells reduced the polysomes to subpolysomes ratio in response to stress, albeit to a lesser extent than wild-type cells (Figure 1D-G, Supplementary Figure S2A, B). This partial dependency on eIF2α phosphorylation is in in agreement with recent reports of *S. pombe* responses to UV and oxidative stress (35,47,48). Accordingly, it has been reported that rapid translational arrest in response to hydrogen peroxide treatment relies on a block in elongation induced by phosphorylation of eukaryotic elongation factor 2 (eEF2), rather than on eIF2α phosphorylation (49). By contrast, the Sty1 protein was not required for the downregulation of translation initiation (Figure 1F, G, Supplementary Figure S2A, B). Indeed, in some cases (H_2O_2 and sorbitol treatments), *sty1Δ* cells reduced translation more than wild type cells (Figure 1G, Supplementary Figure S2A, B). A small reduction in elongation rates is not expected to cause strong changes in polysomes to subpolysomes ratios, and thus may not be discernible from normal translation. However, changes in initiation alone can be easily detected by reductions in polysomes to subpolysomes ratios. Therefore, our polysome profiling data suggest that translation is affected at least at the initiation level upon cadmium, heat shock and H_2O_2 exposure. This effect is only weakly dependent on eIF2α phosphorylation, but is largely independent of MAPK signalling. We also noticed that unstressed *sty1Δ* cells showed higher polysomes to subpolysomes ratios than *eIF2α-S52A* or wild type cells (Figure 1G, Supplementary Figure S2B, S2C). Since Sty1 activation limits eIF2α phosphorylation (10,21), we expected that *sty1Δ* cells would show repressed translation initiation and lower polysomes to subpolysomes ratio. The underlying cause of these higher polysomes might be a general elongation decrease, although other mechanisms cannot be excluded.

Gene-specific translational regulation upon stress exposure

We used ribosome profiling to investigate gene-specific translational control in response to stress. Ribosome-protected fragments (RPFs) were isolated and analysed by high-throughput sequencing, whereas mRNA levels were

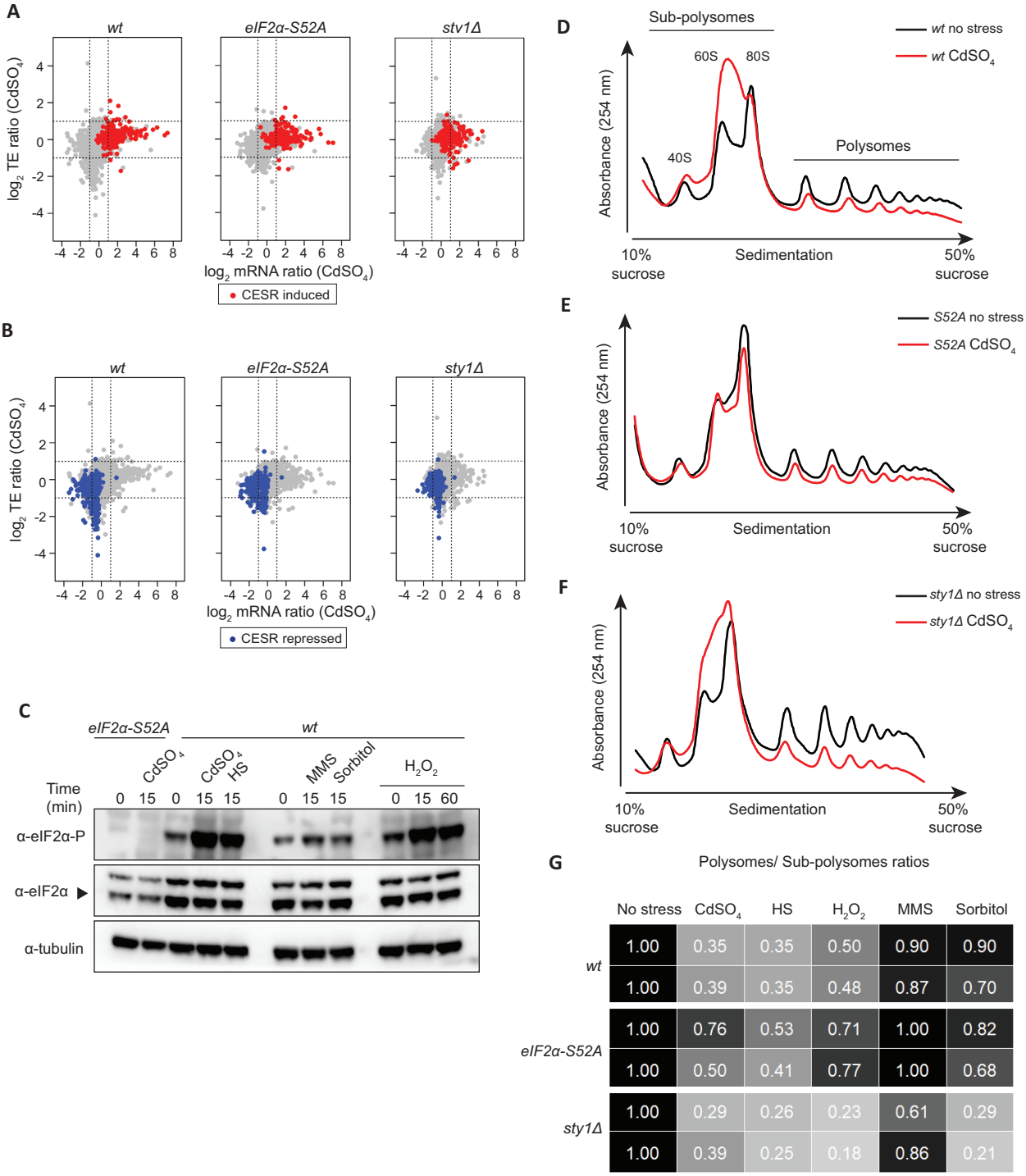

	No stress	$CdSO_4$	HS	H_2O_2	MMS	Sorbitol
wt	1.00	0.35	0.35	0.50	0.90	0.90
	1.00	0.39	0.35	0.48	0.87	0.70
eIF2α-S52A	1.00	0.76	0.53	0.71	1.00	0.82
	1.00	0.50	0.41	0.77	1.00	0.68
sty1Δ	1.00	0.29	0.26	0.23	0.61	0.29
	1.00	0.39	0.25	0.18	0.86	0.21

Figure 1. General responses to stress. (**A**) Scatter plot comparing mRNA levels and translation efficiencies (log_2 ratios stress/control) upon cadmium treatment (15 min) in wild type, *eIF2α-S52A* and *sty1Δ* genetic backgrounds. CESR-induced genes are plotted in red. (**B**) Same dataset as in A, but CESR-repressed genes are highlighted in blue. (**C**) Western blots comparing eIF2α phosphorylation levels after the five treatments for the indicated times in wild type cells. In the first two lanes (left), *eIF2α-S52A* cells were used as negative control for the anti-eIF2α phosphorylation antibody. Tubulin was employed as a loading control. (**D**–**F**) Representative polysome profile traces before and after cadmium treatment (15 min) in wild type (D), *eIF2α-S52A* (E) and *sty1Δ* cells (F). (**G**) Quantification of polysomes to subpolysomes ratios after five stress treatments (15 min). The data are normalised to control unstressed cells. Unnormalized values are presented in Supplementary Figure S2B. The data are shown for two independent biological replicates of each experiment.

estimated in parallel by RNA-seq. The number of RPFs mapped to each coding gene, normalized by the corresponding number of RNA-seq reads, was used to calculate relative translation efficiencies (TEs) (Figure 2A). Note that upregulated TEs reflect increased ribosomal densities on a transcript, which may be caused by higher translation initiation or by decreases in elongation rates (e.g. ribosome stalling). Genes showing significant changes in TE upon stress treatment were identified using RiboDiff (see Methods), with thresholds of a minimum 1.5-fold change and adjusted P value < 0.01 (Supplementary Dataset S6). This approach does not consider global changes in gene expression and, therefore, may overestimate TE values. Nevertheless, these TE values reflect relative changes among conditions and among genetic backgrounds, and identify genes that behave differently from the majority of transcripts.

Upon stress, the number of mRNAs with increased TEs (potentially up-regulated at the translational level) was much smaller than those affected at the transcript level (Table 1). In relative terms, unlike transcriptomic responses, the numbers of genes that showed lower TEs were higher than those with increased TEs (Table 1). Thus, the gene-specific translational response seems to be targeted to reduce mRNA translation. The treatment that had the most widespread effect was cadmium, followed by heat shock and H_2O_2, while fewer changes were detected upon the applied MMS and sorbitol concentrations (Table 1). This trend is generally similar to transcriptional and eIF2α phosphorylation changes (Figure 1C), indicating a correlation among increases in eIF2α phosphorylation, transcriptional programs, and translational regulation.

We found 82 genes with increased TEs in wild type cells in at least one stress treatment, 28 of which overlapped with the CESR induced genes (P value $< 5 \times 10^{-15}$). Of those 82 genes, four were induced in all the stress conditions except for sorbitol, and 15 were shared across cadmium and heat shock. We could not find any specific GO category enriched within the 82 genes (see Materials and Methods). Yet, the data included individual genes that have previously been linked to the stress response. An example of cadmium-upregulated gene (both transcriptionally and at the TE level) is *prr1*, which encodes a transcription factor involved in the oxidative stress response and sexual differentiation (50–52) (Supplementary Figure S3A). This regulation is consistent with the generation of reactive oxygen species after cadmium stress (53). Other interesting genes were related to protein catabolism (*ubp3*, in cadmium and heat shock), autophagy (*atg3*, in cadmium), cell cycle (*srk1*, in cadmium), DNA repair (*dna2*, in heat shock and *uve1*, in H_2O_2 and cadmium), transmembrane transport, carbohydrate and amino acid metabolism. The most TE-upregulated gene was *fil1* (12), which encodes a transcription factor essential for the response to amino acid starvation (Figure 2A). The role of this gene in stress responses is discussed in detail below. Finally, we found that upon cadmium and heat shock treatments, more than 45% of genes with elevated TEs were also transcriptionally induced, whereas <14% of translationally downregulated were also transcriptionally repressed. This coordination of transcriptomic and translational induction (potentiation) has been observed by polysome profiling in budding and fission yeast responses to stress (36,54).

We also identified 382 translationally down-regulated genes (TE repressed in at least one condition), 149 of which were part of the CESR-repressed list (P value $< 5 \times 10^{-73}$). Like the induced genes, cadmium, heat shock and H_2O_2 led to stronger effects, whereas the consequences of MMS and sorbitol exposure were very mild (Table 1). The most extensive overlap was between cadmium and heat shock stress, with 170 genes shared ($P = 10^{-173}$). These genes included *cdr2*, which is involved in the regulation of the G2/M transition through the inhibition of the Wee1 kinase (55) (Supplementary Figure S3B). Repression of this gene is consistent with the block of cell cycle progression in response to stress. There was also a substantial overlap (38 genes) among cadmium, heat shock and H_2O_2 stresses. These data indicate that heavy metal exposure, oxidative conditions and heat shock cause similar translational responses.

Repressed genes at the TE level were mainly associated with cytoplasmic translation (GO:0002181; $P = 10^{-89}$), ribosome biogenesis (GO:0042254; $P = 10^{-28}$) and ribosome assembly (GO:0042255; $P = 10^{-11}$). Consistently, 110 of the 382 down-regulated genes ($P = 10^{-99}$) encoded ribosomal proteins (Figure 2A, B). We have previously observed this effect upon nitrogen depletion (30) and amino acid starvation (12), demonstrating that this is a widespread translational response to stress.

Finally, we investigated whether translational responses were dependent on the major stress response pathways. Many TE-upregulated genes were partially induced in both *eIF2α-S52A* and *sty1Δ* mutants (Figure 2C). However, a direct comparison of the induction levels in wild type and mutant cells (Figure 2D, Supplementary Dataset S7), revealed that the upregulation in the mutants was impaired for most genes. A very similar dependency was observed for downregulated genes (Figure 2E, F), which were generally less repressed in both mutant backgrounds. Therefore, both the eIF2α and the MAPK pathways contribute to a normal translational response, but neither of them is sufficient to explain the response in its entirety.

Fil1 is the major translational responder to stress

The transcription factor *fil1* was very highly induced at the TE level by cadmium, heat shock, and H_2O_2 treatments, while showing small reductions or no changes in mRNA levels (Figure 3A, B). There was also a weak TE induction after MMS treatment, but none after sorbitol. These data mirror the change in eIF2α phosphorylation in these stresses (Figure 1C). Consistently, the TE induction of *fil1* was completely dependent on eIF2α phosphorylation, and very weakly on Sty1 signalling (Figure 3A). We investigated if this increase in TE was accompanied by higher protein levels. To do this, cells expressing Fil1-TAP from their endogenous locus were used to compare protein levels by immunoblot in the five stress conditions. Consistent with the TE data, there was a strong increase in protein levels after cadmium, H_2O_2 and heat shock treatments, lower after MMS, and none upon sorbitol (Figure 3C, D and Supplementary Figure S3C–E). The kinetics of the *fil1* induction

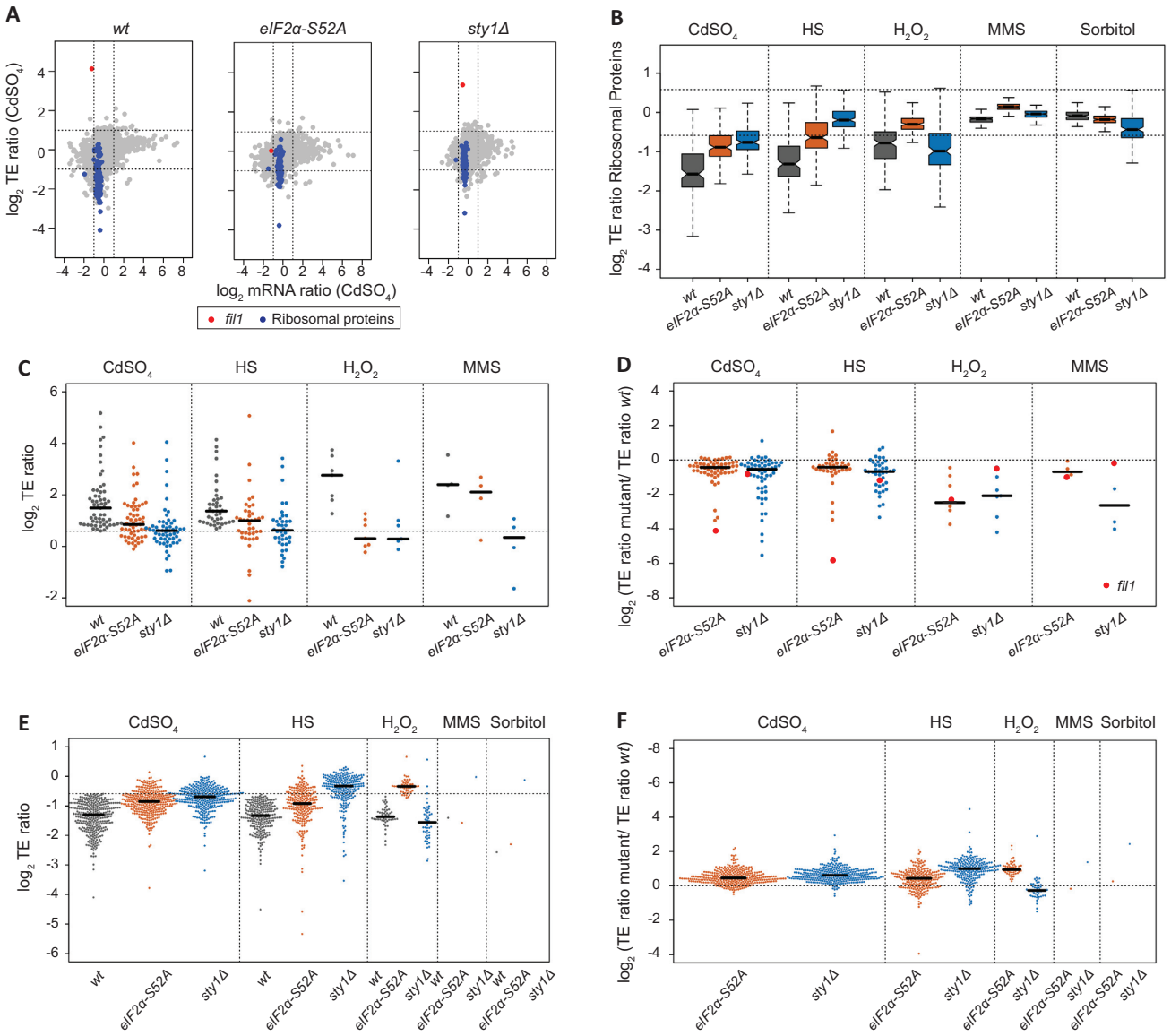

Figure 2. Translational regulation upon stress exposure. (**A**) Scatter plot comparing mRNA levels and translation efficiencies (log_2 ratios stress/control) upon cadmium treatment (15 min) in wild type, *eIF2α-S52A* and *sty1Δ* genetic backgrounds. The *fil1* gene is plotted in red and genes encoding ribosomal proteins in blue. Note that this is the same dataset shown in Figure 1A and B, but with different genes highlighted. (**B**) Boxplots comparing translation efficiencies of stressed and control cells (log_2 ratios stress/control) of genes encoding ribosomal proteins. Data are shown for wild type, *eIF2α-S52A* and *sty1Δ* cells. (**C**) Comparisons of translation efficiencies of stressed (15 min) and control cells (log_2 ratios stress/control). Only genes that showed significant TE upregulation in wild type cells in at least one stress are displayed. Data are presented for wild type, *eIF2α-S52A* and *sty1Δ* cells. (**D**) As in C, but TE changes have been normalised to those of wild type cells. (**E**) As in C, but only genes that showed significant translational downregulation are displayed. Dots corresponding to *fil1* gene are shown in red. (**F**) As in D, but data are displayed for significantly downregulated genes.

was stress-specific, with cadmium and heat shock showing a transient response (peaking at 15 min) and H_2O_2 and MMS showing slower responses. In particular, the increase at 60 min after H_2O_2 and MMS (Figure 3D and Supplementary Figure S3D) was analogous to the behaviour of CESR-induced genes under the same conditions, whose induction persisted for an hour (14). The variety in induction kinetics suggests that Fil1 protein induction may be regulated at other levels in addition to translation. Consistent with the ribosome profiling data, no Fil1 protein induction was detected in *eIF2α-S52A* cells (Figure 3C, D and Supplementary Figure S3C–E). Surprisingly, Fil1 protein levels were higher in *sty1Δ* than in wild type cells, even in the absence of stress (Figure 3C, D and Supplementary Figure S3C–E). This may relate to the fact that *sty1Δ* cells are sensitive to stress (56–59). Indeed cells lacking this protein show evidence of an induced stress response even under normal laboratory growth conditions (14). Taken together, these data indicate that *fil1* translational induction upon stress leads to an increase in Fil1 protein levels in an eIF2α-dependent manner, and that the Sty1 MAPK pathway modulates this effect. This response takes place in rich medium, where Fil1 is not required for normal growth (12). Therefore, Fil1 behaves as a general stress-responsive transcription factor.

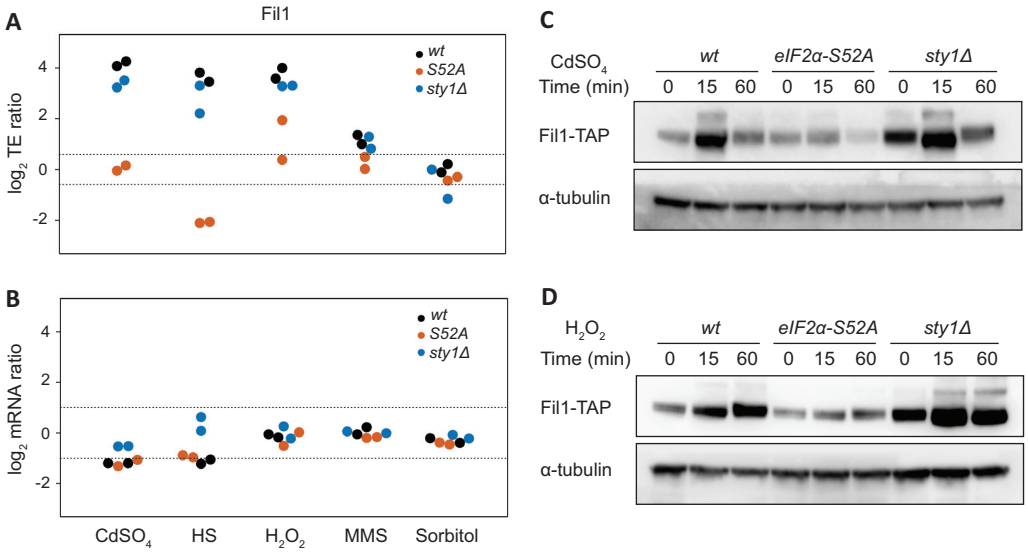

Figure 3. *Fil1* is the major translational responder to stress. (**A**) Comparison of translation efficiency of the *fil1* gene between stressed and control cells ($\log_2$ ratios stress/control). The dotted lines indicate 1.5-fold changes. Data are presented for wild type, *eIF2α-S52A* and *sty1Δ* cells. (**B**) As in C, but for *fil1* mRNA changes. The dotted lines indicate 2-fold changes. (**C**) Western blots to measure Fil1-TAP protein levels after cadmium treatment for the indicated times. Data are presented for wild type, *eIF2α-S52A* and *sty1Δ* cells. Tubulin was used as a loading control. (**D**) As in C, but after H_2O_2 treatment.

We then investigated the role of Fil1 in the transcriptional responses to stress. We performed RNA-seq experiments in the five stress conditions in cells lacking *fil1*, and monitored the behaviour of 165 previously identified Fil1 targets (12). Note that Fil1 targets were defined as genes that showed lower expression in *fil1Δ* cells in minimal medium and in the absence of stress (12). In unstressed cells growing in rich medium, Fil1 targets were expressed at slightly lower levels in the *fil1Δ* mutant (Figure 4A–C). In response to cadmium, heat shock and H_2O_2 treatments, Fil1 targets were expressed at substantially decreased levels in the mutant (Figure 4A–C and Supplementary Figure S4A–E). Consistently, Fil1 target genes overlapped significantly with genes underexpressed in *fil1Δ* cells at 15 min after heat shock (Figure 4D), and with genes underexpressed 60 min after H_2O_2 treatment (Figure 4E). These data demonstrate that Fil1 promotes the expression of a common group of genes in response to cadmium, heat shock and H_2O_2 treatments.

These results suggest that Fil1 may be important for survival to stress in rich medium. We explored this hypothesis by performing viability assays of wild type and *fil1Δ* mutant under the five stress treatments (Supplementary Figure S5). *fil1Δ* cells were sensitive to high temperature, H_2O_2 and MMS, whereas no difference to wild-type was observed at the sorbitol concentrations applied. Surprisingly, cells lacking Fil1 were resistant to cadmium treatment (Supplementary Figure S5). Although the reason for this phenotype is unclear, deletion of genes encoding other transcription factors involved in stress responses (*atf1, prr1*) (50,60,61), and of genes encoding several RNA-binding proteins (62) lead to similar resistance to cadmium.

As mentioned above, Fil1 is necessary for the normal expression of its targets in response to several stresses (Figure 4A–C), and Fil1 expression was induced under the same conditions in an eIF2α-dependent manner (Figure 3C, D and Supplementary Figure S3C). To investigate if *fil1* induction is required for the normal expression of Fil1 targets, we compared the expression levels of *fil1* targets upon stress in wild type and eIF2α-S52A mutants. After 15 min of treatment, Fil1 target levels were mildly increased by heat shock and H_2O_2 (but not by cadmium) in an eIF2α-dependent manner (Figure 4F). As Fil1 targets tend to be induced more strongly by H_2O_2 at later time points (Figure 4C), we repeated the experiment upon a 60-min H_2O_2 exposure. Indeed, this led to a late and stronger induction of Fil1 targets that was almost completely dependent on eIF2α phosphorylation (Figure 4G). Consistently, we found a significant overlap between Fil1 targets and those transcripts underexpressed in *eIF2α-S52A* cells relative to wild type cells (Table 2) after cadmium ($P = 7 \times 10^{-3}$), H_2O_2 ($P = 2 \times 10^{-6}$) and heat shock treatments ($P = 5 \times 10^{-46}$). These results indicate that, at least in some conditions, *fil1* translational upregulation plays a role in the implementation of the normal transcriptional responses to stress.

In addition, cells lacking Sty1 showed increased mRNA levels of Fil1 targets in both stressed and unstressed cells (Figure 4H). Indeed, there were significant overlaps between Fil1 target genes and upregulated genes in unstressed *sty1Δ* cells ($P = 4.9 \times 10^{-11}$), and between Fil1 targets and upregulated genes under stress conditions in *sty1Δ* cells relative to wild type cells (highest $P < 8.5 \times 10^{-3}$ in H_2O_2 induced list). These data are also consistent with the increased Fil1 protein levels in unstressed *sty1Δ* cells (Figure 3C, D and Supplementary Figure S3C–E). These data suggest that the Sty1 MAPK pathway cross-talks with the Integrated Stress Response, consistent with previous observations (10,21).

Ribosome occupancy on tryptophan codons is increased upon oxidative stress

Ribosome profiling provides information on ribosome locations with codon-level resolution and can thus be used to detect codon-specific ribosome stalling caused by stress

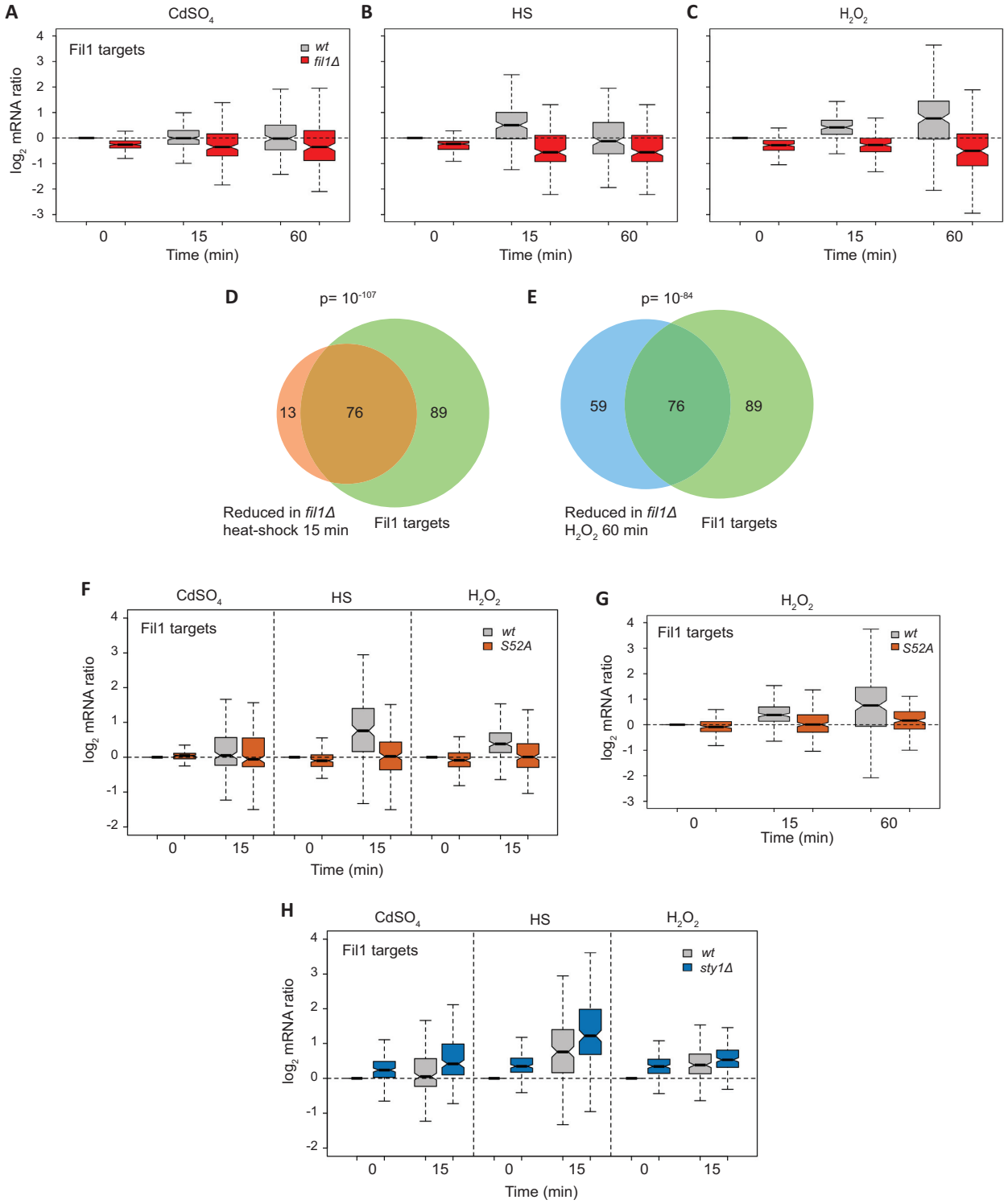

Figure 4. Role of Fil1 in the transcriptional responses to stress. (**A–C**) Boxplots comparing mRNA levels of stressed and control cells (log_2 ratios stress/control) of Fil1 targets. Data are shown for wild type and *fil1Δ* cells at the indicated times and stresses. (**D**) Venn diagram showing the overlap between genes expressed at lower levels in *fil1Δ* mutant relative to wild type cells after heat shock (15 min), and Fil1 targets in unstressed cells. The *P* value of the observed overlap is shown. (**E**) As in D, but genes expressed at lower levels in *fil1Δ* mutant relative to wild type after H_2O_2 treatment (60 min) were compared to Fil1 targets in unstressed cells. (**F**) As in A to C, but after cadmium, heat shock and H_2O_2 treatments, in wild type and *eIF2α-S52A* strains. (**G**) As in F, but after H_2O_2 treatment and with an additional time point. (**H**) As in F, but in the wild type and *sty1Δ* strains.

conditions (12). To investigate this level of regulation, we quantified the fraction of ribosomes translating each of the 61 amino acid-encoding codons, normalized by the abundance of the corresponding codon in the transcriptome. This 'relative codon occupancy' reflects the average time spent by the ribosome on each codon. The single codon for tryptophan (UGG) showed strongly increased ribosome occupancy upon H_2O_2 treatment (Figure 5A and Supplementary Figure S6A). This enrichment was highly specific, as it was not observed for any other codon, and in any other stress condition (Supplementary Figure S6B).

We then explored the possibility that ribosome stalling on tryptophan codons leads to accumulation of ribosomes (ribosome queuing). We monitored the transcriptome-wide average density of RPFs on and around each of the 61 amino acid-encoding codons. As expected, there was a clear peak of RPFs specific to both tryptophan codons and H_2O_2 treatment (Figure 5B and Supplementary Figure S6C). Interestingly, we also observed peaks of RPFs 10 and 20 codons upstream of tryptophan codons in cells subjected to oxidative stress (Figure 5B and Supplementary Figure S6C). These peaks were also present in *eIF2α-S52A* cells (Supplementary Figure S6D). As ribosomes typically protect a fragment of 30 nucleotides, these are very likely to represent ribosomes queuing immediately upstream of ribosomes stalled on tryptophan codons. The accumulation of RPFs on UGG codons could also be observed for individual transcripts (*arg1* and *leu3*, Supplementary Figure S7A–D).

A possible explanation for the stalled ribosomes was that cellular tryptophan levels decreased because of the H_2O_2 treatment. We therefore measured intracellular amino acid concentrations by mass spectrometry. We observed a reduction of ∼20% in tryptophan levels. However, this change was borderline of statistically significance ($P = 0.04$), and was smaller than that of other amino acids that did not show any difference in ribosome occupancy of their cognate codons (Figure 5C, Supplementary Figure S7E).

A second hypothesis was that the levels of tRNA charging could be affected by oxidative stress. To investigate this possibility, we compared the levels of amino-acylated (charged) and deacylated (uncharged) tRNA-Trp. tRNAs were first subjected to periodate oxidation. This treatment leads to the removal of the 3′ nucleotide of uncharged tRNAs through β-elimination, whereas the charged fraction is protected by the amino acid and remains unaltered. The tRNAs are then deacylated at high pH. Thus, uncharged and charged tRNAs show a difference of one nucleotide in size, which can be detected by polyacrylamide gel electrophoresis and Northern blotting (39) (Figure 5D, E). An increase in the ribosome occupancy of some codons in *S. cerevisiae* after oxidative stress has been reported (63), but the underlying mechanism involves tRNA fragmentation. However, we used tRNA-Trp deacylated samples as controls and showed that total levels of tRNA-Trp were not affected by oxidative stress, ruling out the fragmentation of tRNAs (27) (Figure 5D). By contrast, tRNA-Trp charging levels were significantly reduced after H_2O_2 treatment (Figure 5D, E). To confirm that this effect is specific of tRNA-Trp, we verified that charged tRNA-His levels remained identical upon H_2O_2 treatment (Figure 5F, G). The addition of supplemental tryptophan to rich medium 2 h before, or only during the H_2O_2 treatment, prevented the charged tRNA-Trp drop and increased the charging levels (Figure 5H, I). Moreover, ribosome profiling showed that the increase in codon occupancy and ribosome stalling at the UGG codon were lost after the addition of tryptophan (Figure 5J, K and Supplementary Figure S7C, D). Thus, these data indicate that the increase in ribosome occupancy at the tryptophan codon in H_2O_2 stress condition reflects a reduced charged tRNA-Trp fraction. The direct cause of this phenomenon is unclear. mRNA levels and TE of the tRNA-Trp ligase, encoded by *wrs1* gene, remained unaffected by H_2O_2 exposure. We also verified that the Wrs1 protein levels were not affected by H_2O_2 treatment (Supplementary Figure S7F).

Decreased tRNA-Trp charging may affect eIF2α phosphorylation

In *S. cerevisiae* uncharged tRNAs activate the Gcn2 kinase, which phosphorylates eIF2α to downregulate global translation initiation in response to amino acid starvation (7). Recently, it has been shown that Gcn2 in *S. pombe* is activated in response to UV and oxidative stress through a mechanism that involves Gcn1 and most likely the binding of tRNAs (64). Thus, we reasoned that increased levels of uncharged tRNA-Trp upon H_2O_2 treatment might contribute to eIF2α phosphorylation. To explore this possibility, we compared eIF2α phosphorylation levels upon H_2O_2 stress in the presence and absence of supplemental tryptophan. Consistent with this idea, addition of tryptophan (which increases tRNA-Trp charging levels, see above) caused a reduction of eIF2α phosphorylation (Figure 6A, B, Supplementary Figure S8). These data suggest that uncharged tRNA-Trp could promote Integrated Stress Response signalling upon H_2O_2 exposure, and thus affect both translation initiation and translation elongation. Surprisingly, the polysomes to subpolysomes ratio was unaffected by exogenously added tryptophan (Supplementary Figure S9A, B). One explanation is that the loss of ribosome stalling (which would reduce the polysome to subpolysomes ratio) is counteracted by an increase in translation initiation rates, which would increase this ratio.

We also found that tryptophan in the culture medium did not affect cell growth or survival under oxidative stress conditions (Supplementary Figure S9C–E). These results suggest that the block on translation elongation has a subtle impact on cells, and the effects may be related to the fine-tuning of the oxidative stress response at the translation level.

Differences in charged tRNA-Trp levels cannot affect codon usage because tryptophan is encoded by only one codon, UGG. However, as tryptophan is the least frequent amino acid in proteins (<0.015% on average), we asked whether the translation efficiency of genes containing more tryptophan might be affected by lower charged tRNA-Trp levels upon H_2O_2 stress. Genes were ranked by the percentage of tryptophan codons in their coding sequences, and assigned to 11 bins. We then measured the apparent change in translation efficiency upon oxidative stress for each bin. The data showed a trend towards increased translation efficiency changes after H_2O_2 treatment with higher tryp-

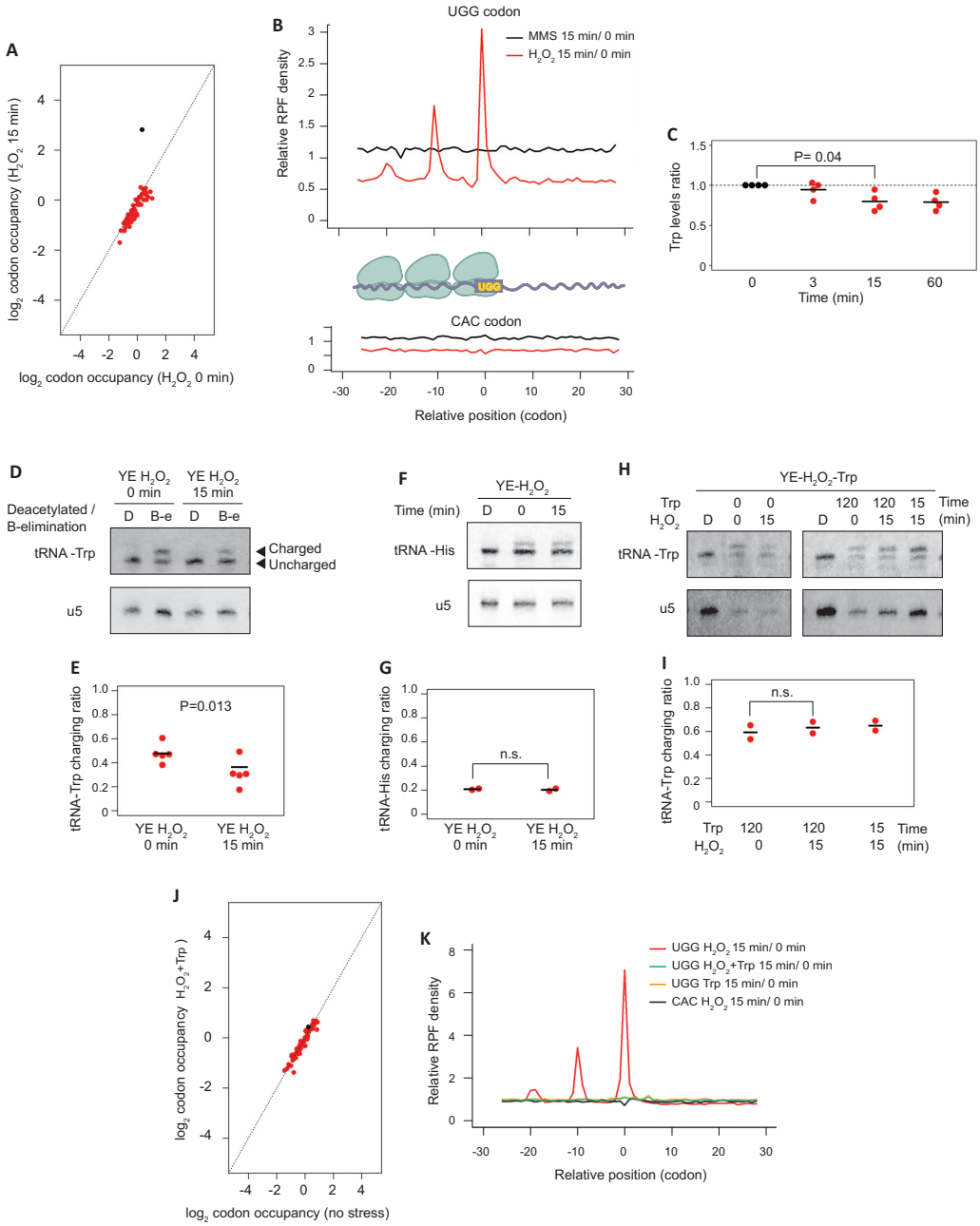

Figure 5. Levels of charged tRNA-Trp are affected by oxidative stress. (**A**) Scatter plots showing $\log_2$ relative codon occupancies before and after H_2O_2 treatment for 15 min in wild type cells. The dot corresponding to UGG codon encoding tryptophan is shown in black. (**B**) Metagene depicting average read density of RPFs around tryptophan codons (UGG) or one of the histidine codons (CAC). The cartoon shows the interpretation of the results of the experiment, with ribosomes queuing upstream of the tryptophan codon-stalled ribosome. (**C**) Changes in intracellular tryptophan levels in response to H_2O_2 exposure. Tryptophan levels were measured at the indicated times after H_2O_2 addition to the culture medium. Each dot corresponds to an independent biological replicate ($n = 4$), and the horizontal lines indicate the means. No adjustment for multiple testing was performed. (**D**) Representative northern blot for the determination of tRNA-Trp charging levels before and after H_2O_2 exposure. The top blot was hybridised with a probe against tRNA-Trp, and the bottom one with a probe against the U5 snRNA. In the upper blot, the top band corresponds to charged tRNA, and the bottom to the uncharged form. tRNA-Trp samples were either deacylated to remove the linked amino acid from charged tRNAs (sample D) or oxidised to remove the unprotected 3′ nucleotides from uncharged tRNAs by beta-elimination (sample B–E) (see Materials and Methods for details). U5 snRNA was used as a loading control. (**E**) Quantification of tRNA-Trp charging ratios from experiment D. Ratios between charged and uncharged tRNA were calculated. Each dot corresponds to an independent biological replicate ($n = 5$), and the horizontal line indicates the mean. (**F**) As in D, but using a probe against tRNA-His (top panel) or U5 snRNA (bottom). (**G**) Quantification of tRNA-His charging from the experiment shown in F (n = 2 independent replicates). (**H**) Northern blot as in D, to explore the effects of supplementing the culture medium with tryptophan. Cells were grown in the presence of tryptophan for 0, 15 or 120 min, and H_2O_2 was added at the indicated times (0, 15 min) before the end of the incubation with tryptophan. Control deacylated RNA (sample D) is used to identify the location of uncharged tRNA. (**I**) Quantification of tRNA-Trp charging levels from experiment H, right panels ($n = 2$ independent replicates). (**J**) Scatter plots showing $\log_2$ relative codon occupancies before and after H_2O_2 and tryptophan treatment for 15 min in wild type cells. The dot corresponding to the UGG codon, encoding tryptophan, is shown in black. (**K**) Metagene depicting average read density of RPFs around tryptophan codons (UGG) or one of the histidine codons (CAC) in different conditions.

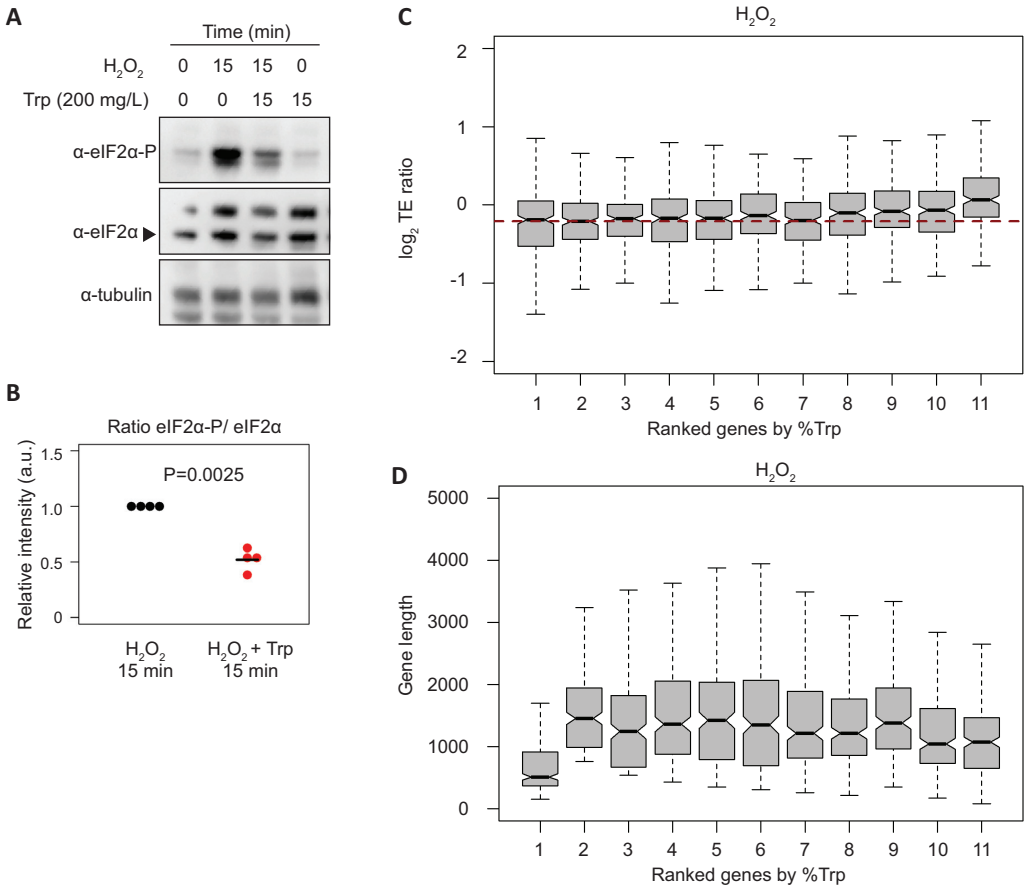

Figure 6. Oxidative stress affects the translation efficiency of tryptophan codon-enriched genes, and decreased tRNA-Trp charging may affect eIF2α phosphorylation. (**A**) Western blots to investigate the effect of tryptophan on eIF2α phosphorylation levels after H_2O_2 treatment. Cells were treated with H_2O_2 for 15 min and supplemental tryptophan was added as indicated. Tubulin was used as a loading control. (**B**) Quantification of eIF2α phosphorylation normalized to total eIF2α from the experiment shown in A ($n = 4$ independent replicates). (**C**) Boxplots showing changes in translation efficiency upon oxidative stress ($\log_2$ TE ratios stress/control, 15 min treatment) according to tryptophan codon content. Genes were binned into 11 categories based on the fraction of tryptophan codons in their coding sequences (the first group contains 269 genes without tryptophan, codons and the other 10 groups have 234 genes each). The horizontal red dashed line indicates the median of the second group. (**D**) As above, but displaying coding sequence lengths.

tophan codon content, which was not observed in other stresses (Figure 6C and Supplementary Figure S10A–D) or in other codons (Supplementary Figure S10E, F). We also ruled out that this trend was determined by transcript lengths (Figure 6D and Supplementary Figure S10G, H). The group of genes lacking tryptophan codons is enriched in genes encoding ribosomal proteins ($P = 10^{-27}$), which have a small transcript size (Figure 6D). By contrast, the group with the most tryptophan (0.023–0.056%) showed an enrichment in genes related to lipid biosynthesis (GO:0008610; $P = 6.6 \times 10^{-10}$), protein glycosylation (GO:0006486; $P = 4 \times 10^{-7}$) and cell wall biogenesis (GO:0071554; $P = 1.5 \times 10^{-5}$). This enrichment is consistent with the fact that tryptophan is an amphipathic amino acid, often found in transmembrane domains. Given that translation efficiency as defined above is a relative measurement of the number of ribosomes per transcript (normalised to mRNA abundance), an increase in this parameter in tryptophan codon-rich genes is likely to reflect a slowdown of translation elongation of these genes rather than an increase in their protein synthesis. Thus, we propose that oxidative stress modulates translation at two levels: at initiation, through the Integrated Stress Response, and at elongation, through tryptophan codon stalling.

DISCUSSION

The translational landscape of the response to multiple stresses

We present a genome-wide analysis of the translational response of the fission yeast *S. pombe* to five different stresses. We found a clear correlation among the extent of transcriptional responses, increased levels of eIF2α phosphorylation, pronounced global downregulation of translation and induction of *fil1* translation. Of course, as we monitored a single time point and condition for each stress, the conclusions about the relative strength of the effects are only valid to the specific experimental conditions used. Despite this caveat, our results indicate that the translational response to stress is mainly directed to repress the translational machinery, with few genes upregulated at this level. Moreover, we found that many differentially translated genes are often regulated in multiple stresses. Thus, our study provides

useful information about the stress response at the translational level and insight into the biological response to stress.

Fil1 regulation and role in stress responses

The induction of the Fil1 transcription factor in multiple stress conditions in rich medium was noteworthy, as Fil1 is a master regulator of the amino acid starvation response (analogous to Gcn4 and Atf4), and is required to maintain a normal growth rate in minimal medium (12). Cells lacking Fil1 showed similar growth than wild type cells in rich medium, suggesting that Fil1 does not have a role in unstressed cells in rich medium. The *fil1* gene showed much higher translational induction upon cadmium, heat shock and H_2O_2 in rich medium than in amino acid starvation induced by 3-AT in minimal medium (17-fold, 12-fold, 13-fold and 3.8-fold, respectively). A possible explanation is that *fil1* translation levels may already be higher in minimal medium in unstressed cells. Similarly, the induction of the Fil1 orthologue in *S. cerevisiae* (Gcn4) has been reported not only in amino acid starvation or glucose limitation, but also after MMS (although the conditions were different from the ones used in this work) and H_2O_2 treatments (33,34,65). These results suggest that metabolic adaptation, mediated by translationally controlled transcription factors such as Fil1 and Gcn4, is an evolutionary conserved part of many stress responses (and not just amino acid starvation).

Fil1-dependent genes are mostly related to amino acid metabolism and transmembrane transport, and show a significant overlap with CESR induced genes. In rich medium, cells lacking Fil1 are unable to regulate the expression of Fil1 targets after cadmium, heat shock and H_2O_2 treatments. In addition, this regulation is also impaired in *eIF2α-S52A* cells, consistent with the complete absence of *fil1* induction. Surprisingly, Fil1 and its targets were upregulated in *sty1Δ* cells (compared to wild type) in unstressed conditions, possibly because the lack of a normal transcriptional response in these cells may lead to stress (14). Moreover, *sty1Δ* cells are sensitive to stress (56–59). This may also reflect that Sty1 may have a role in the modulation of eIF2α kinases after stress. Indeed, *sty1Δ* cells show increased eIF2α phosphorylation after oxidative stress, which might result in induction of Fil1 (10,21). Given that Sty1 is also important in adaptation to stress and that nothing is known about Fil1 protein stability or post-translational modifications, it could be also involved in downregulation of Fil1 after stress.

Upon cadmium treatment, despite the induction of Fil1, the expression of Fil1-dependent genes in wild-type cells is very weak and *fil1Δ* cells are resistant to this stress. Cadmium stress increases ROS and intracellular oxidative stress (53), but the response is very different from H_2O_2 treatment. For example, cadmium is imported through specific transporters, whereas H_2O_2 freely diffuses into cells. Moreover, H_2O_2 converts into superoxide, and is a substrate for the peroxiredoxin system that is responsible for the oxidation of most proteins. Indeed, *S. pombe* cells lacking transcription factors like Atf1 or Prr1 are sensitive to H_2O_2, but resistant or insensitive to cadmium (50,61). Additionally, Fil1 may drive the response to amino acid starvation partially through the action of downstream transcription factors (12). Thus, different kinetics in the induction and the expression of Fil1-dependent genes suggest that Fil1 might be modulating transcriptional changes depending on the stress through other transcription factors. We propose that Fil1 acts as a master regulator of several stress conditions, promoting a distinct response for each situation. Further work will be required to unveil the direct targets of Fil1 under each stress condition, and whether Fil1 can activated the in different ways to modulate specific responses.

Ribosomes stall on tryptophan codons upon H_2O_2 treatment, leading to ribosome queuing

Ribo-seq experiments revealed that oxidative stress caused ribosome stalling on tryptophan codons, which correlated with decreased levels of charged tRNA-Trp. By contrast, intracellular levels of tryptophan were not changed significantly under these conditions, suggesting that tryptophan metabolism is not strongly affected by the stress. However, not all amino acids limitations promote the deacylation of the corresponding tRNA and ribosome pausing (66), and other tRNAs species can become deacylated faster than tRNAs charged with the starved amino acid (67). Therefore, we cannot completely rule out that slight changes in intracellular levels of tryptophan lead to tRNA-Trp deacylation. Other possible explanations are that changes in tRNA modifications, or in the tRNA-Trp synthetase activity, may affect the levels of charged tRNA-Trp and cause stalling. An example of modulation of the tRNA-Trp synthetase activity under conditions of oxidative stress has been reported in humans (68).

Although we were unable to detect changes in viability of wild type cells upon oxidative stress in the presence of supplemental tryptophan, we hypothesize that ribosome stalling on tryptophan codon may have an effect on fine-tuning translational rates. Indeed, it has been proposed that translational pausing at rare codons might provide a time delay to facilitate proper protein folding (69,70). We also report that ribosome stalling on a rare codon leads to ribosome queuing (Figure 5B). Indeed, we detect accumulations of up to three ribosomes (including the tryptophan codon-stalled ribosome). These results suggest that ribosome stalling can affect translation elongation by blocking the passage of translating upstream ribosomes.

The main eIF2α kinase activated in response to early exposure to H_2O_2 in *S. pombe* is Gcn2 (10). The molecular pathway leading to activation of Gcn2 upon nutrition limitation is well understood: Gcn2 is activated by uncharged tRNAs, which bind the histidyl-tRNA synthetase-related domain of Gcn2 at the C-terminus (71–73). However, Gcn2 is activated by other stresses that are not expected to cause uncharged tRNA accumulation (64), such as UV irradiation or oxidative stress. Under these conditions, the tRNA binding domain of Gcn2 is still required for its activation (64). In addition, it has been recently shown that ribosome collisions induce eIF2α phosphorylation by Gcn2 in an uncharged-tRNA independent manner in mammalian cells, suggesting that there is a regulatory mechanism linking translation elongation and initiation (74,75).

Here, we provide evidence that a nutrient-unrelated stress like oxidative stress causes uncharged tRNA accumulation.

In addition, we show that eIF2α phosphorylation after oxidative stress correlates with uncharged tRNA-Trp accumulation. Addition of tryptophan reverses ribosome stalling on tryptophan codons and results in a reduction in the levels of both uncharged tRNA-Trp and of eIF2α phosphorylation. Thus, we propose that the accumulation of uncharged tRNA-Trp upon oxidative stress, which causes an elongation defect, is used to regulate initiation through Gcn2 activation.

DATA AVAILABILITY

All raw data files have been deposited in ArrayExpress (76) [https://www.ebi.ac.uk/arrayexpress/] under accessions: E-MTAB-8746, E-MTAB-8686, E-MTAB-8744, E-MTAB-8745, E-MTAB-8602 and E-MTAB-8583.

SUPPLEMENTARY DATA

Supplementary Data are available at NAR Online.

ACKNOWLEDGEMENTS

We thank Samuel Marguerat and Caia Duncan for comments on the manuscript and Mathew Peacey and Anno Koetje for help with experiments.

FUNDING

Biotechnology and Biological Sciences (BBSRC) [BB/N007697/1 to J.M.]; Markus Ralser was supported by the Francis Crick Institute, which receives its core funding from Cancer Research UK [FC001134]; UK Medical Research Council [FC001134]; Wellcome Trust [FC001134], as well as specific project funding from the Wellcome Trust [IA 200829/Z/16/Z to M.R.]; German Federal Ministry of Education and Research (BMBF) as part of the National Research Node Mass Spectrometry in Systems Medicine [MSCoreSys 031L0220A]. Funding for open access charge: University of Cambridge.
Conflict of interest statement. None declared.

REFERENCES

1. Spriggs,K.A., Bushell,M. and Willis,A.E. (2010) Translational regulation of gene expression during conditions of cell stress. *Mol. Cell*, **40**, 228–237.
2. Lindqvist,L.M., Tandoc,K., Topisirovic,I. and Furic,L. (2018) Cross-talk between protein synthesis, energy metabolism and autophagy in cancer. *Curr. Opin. Genet. Dev.*, **48**, 104–111.
3. Tahmasebi,S., Khoutorsky,A., Mathews,M.B. and Sonenberg,N. (2018) Translation deregulation in human disease. *Nat. Rev. Mol. Cell Biol.*, **19**, 791–807.
4. Sonenberg,N. and Hinnebusch,A.G. (2009) Regulation of translation initiation in eukaryotes: mechanisms and biological targets. *Cell*, **136**, 731–745.
5. Pavitt,G.D., Ramaiah,K.V.A., Kimball,S.R. and Hinnebusch,A.G. (1998) eIF2 independently binds two distinct eIF2b subcomplexes that catalyze and regulate guanine-nucleotide exchange. *Genes Dev.*, **12**, 514–526.
6. Dever,T.E., Kinzy,T.G. and Pavitt,G.D. (2016) Mechanism and regulation of protein synthesis in Saccharomyces cerevisiae. *Genetics*, **203**, 65–107.
7. Dever,T.E., Feng,L., Wek,R.C., Cigan,A.M., Donahue,T.F. and Hinnebusch,A.G. (1992) Phosphorylation of initiation factor 2α by protein kinase GCN2 mediates gene-specific translational control of GCN4 in yeast. *Cell*, **68**, 585–596.
8. Hinnebusch,A.G. (2005) Translational regulation of Gcn4 and the general amino acid control of yeast. *Annu. Rev. Microbiol.*, **59**, 407–450.
9. Zhan,K., Narasimhan,J. and Wek,R.C. (2004) Differential activation of eIF2 kinases in response to cellular stresses in Schizosaccharomyces pombe. *Genetics*, **168**, 1867–1875.
10. Berlanga,J.J., Rivero,D., Martín,R., Herrero,S., Moreno,S. and De Haro,C. (2010) Role of mitogen-activated protein kinase Sty1 in regulation of eukaryotic initiation factor 2α kinases in response to environmental stress in Schizosaccharomyces pombe. *Eukaryot. Cell*, **9**, 194–207.
11. Martin,R., Berlanga,J.J. and de Haro,C. (2013) New roles of the fission yeast eIF2 kinases Hri1 and Gcn2 in response to nutritional stress. *J. Cell Sci.*, **126**, 3010–3020.
12. Duncan,C.D.S., Rodríguez-López,M., Ruis,P., Bähler,J. and Mata,J. (2018) General amino acid control in fission yeast is regulated by a nonconserved transcription factor, with functions analogous to Gcn4/Atf4. *Proc. Natl. Acad. Sci. U.S.A.*, **115**, E1829–E1838.
13. Vattem,K.M. and Wek,R.C. (2004) Reinitiation involving upstream ORFs regulates ATF4 mRNA translation in mammalian cells. *Proc. Natl. Acad. Sci. U.S.A.*, **101**, 11269–11274.
14. Chen,D., Toone,W.M., Mata,J., Lyne,R., Burns,G., Kivinen,K., Brazma,A., Jones,N. and Bähler,J. (2003) Global transcriptional responses of fission yeast to environmental stress. *Mol. Biol. Cell*, **14**, 214–229.
15. Chen,D., Wilkinson,C.R.M., Watt,S., Penkett,C.J., Toone,W.M., Jones,N. and Rg Bähler,J. (2008) Multiple pathways differentially regulate global oxidative stress responses in fission yeast. *Mol. Biol. Cell*, **19**, 308–317.
16. Toone,W.M. and Jones,N. (1998) Stress-activated signalling pathways in yeast. *Genes Cells*, **3**, 485–498.
17. Shiozaki,K. and Russell,P. (1996) Conjugation, meiosis, and the osmotic stress response are regulated by Spc1 kinase through Atf1 transcription factor in fission yeast. *Genes Dev.*, **10**, 2276–2288.
18. Wilkinson,M.G., Samuels,M., Takeda,T., Mark Toone,W., Shieh,J.C., Toda,T., Millar,J.B.A. and Jones,N. (1996) The Atf1 transcription factor is a target for the Sty1 stress-activated MAP kinase pathway in fission yeast. *Genes Dev.*, **10**, 2289–2301.
19. Gaits,F., Degols,G., Shiozaki,K. and Russell,P. (1998) Phosphorylation and association with the transcription factor Atf1 regulate localization of Spc1/Sty1 stress-activated kinase in fission yeast. *Genes Dev.*, **12**, 1464–1473.
20. Perez,P. and Cansado,J. (2010) Cell integrity signaling and response to stress in fission yeast. *Curr. Protein Pept. Sci.*, **11**, 680–692.
21. Dunand-Sauthier,I., Walker,C.A., Narasimhan,J., Pearce,A.K., Wek,R.C. and Humphrey,T.C. (2005) Stress-activated protein kinase pathway functions to support protein synthesis and translational adaptation in response to environmental stress in fission yeast. *Eukaryot. Cell*, **4**, 1785–1793.
22. Asp,E., Nilsson,D. and Sunnerhagen,P. (2008) Fission yeast mitogen-activated protein kinase Sty1 interacts with translation factors. *Eukaryot. Cell*, **7**, 328–338.
23. Pan,T. (2018) Modifications and functional genomics of human transfer RNA. *Cell Res.*, **28**, 395–404.
24. Jackman,J.E. and Alfonzo,J.D. (2013) Transfer RNA modifications: nature's combinatorial chemistry playground. *Wiley Interdiscip. Rev. RNA*, **4**, 35–48.
25. Kadaba,S., Krueger,A., Trice,T., Krecic,A.M., Hinnebusch,A.G. and Anderson,J. (2004) Nuclear surveillance and degradation of hypomodified initiator tRNAMet in S. cerevisiae. *Genes Dev.*, **18**, 1227–1240.
26. Patil,A., Chan,C.T.Y., Dyavaiah,M., Rooney,J.P., Dedon,P.C. and Begley,T.J. (2012) Translational infidelity-induced protein stress results from a deficiency in Trm9-catalyzed tRNA modifications. *RNA Biol.*, **9**, 990–1001.
27. Thompson,D.M., Lu,C., Green,P.J. and Parker,R. (2008) tRNA cleavage is a conserved response to oxidative stress in eukaryotes. *RNA*, **14**, 2095–2103.

28. Ivanov,P., Emara,M.M., Villen,J., Gygi,S.P. and Anderson,P. (2011) Angiogenin-induced tRNA fragments inhibit translation initiation. *Mol. Cell*, **43**, 613–623.
29. Ingolia,N.T., Ghaemmaghami,S., Newman,J.R.S. and Weissman,J.S. (2009) Genome-wide analysis in vivo of translation with nucleotide resolution using ribosome profiling. *Science*, **324**, 218–223.
30. Duncan,C.D.S. and Mata,J. (2017) Effects of cycloheximide on the interpretation of ribosome profiling experiments in Schizosaccharomyces pombe. *Sci. Rep.*, **7**, 10331.
31. Gerashchenko,M.V., Lobanov,A.V. and Gladyshev,V.N. (2012) Genome-wide ribosome profiling reveals complex translational regulation in response to oxidative stress. *Proc. Natl. Acad. Sci. U.S.A.*, **109**, 17394–17399.
32. Lackner,D.H., Beilharz,T.H., Marguerat,S., Mata,J., Watt,S., Schubert,F., Preiss,T. and Bähler,J. (2007) A network of multiple regulatory layers shapes gene expression in fission yeast. *Mol. Cell*, **26**, 145–155.
33. Mascarenhas,C., Edwards-Ingram,L.C., Zeef,L., Shenton,D., Ashe,M.P. and Grant,C.M. (2008) Gcn4 is required for the response to peroxide stress in the yeast Saccharomyces cerevisiae. *Mol. Biol. Cell*, **19**, 2995–3007.
34. Natarajan,K., Meyer,M.R., Jackson,B.M., Slade,D., Roberts,C., Hinnebusch,A.G. and Marton,M.J. (2001) Transcriptional profiling shows that Gcn4p is a master regulator of gene expression during amino acid starvation in yeast. *Mol. Cell. Biol.*, **21**, 4347–4368.
35. Shenton,D., Smirnova,J.B., Selley,J.N., Carroll,K., Hubbard,S.J., Pavitt,G.D., Ashe,M.P. and Grant,C.M. (2006) Global translational responses to oxidative stress impact upon multiple levels of protein synthesis. *J. Biol. Chem.*, **281**, 29011–29021.
36. Preiss,T., Baron-Benhamou,J., Ansorge,W. and Hentze,M.W. (2003) Homodirectional changes in transcriptome composition and mRNA translation induced by rapamycin and heat shock. *Nat. Struct. Biol.*, **10**, 1039–1047.
37. Moreno,S., Klar,A. and Nurse,P. (1991) Molecular genetic analysis of fission yeast Schizosaccharomyces pombe. *Methods Enzymol.*, **194**, 795–823.
38. Mülleder,M., Bluemlein,K. and Ralser,M. (2017) A high-throughput method for the quantitative determination of free amino acids in saccharomyces cerevisiae by hydrophilic interaction chromatography-tandem mass spectrometry. *Cold Spring Harb. Protoc.*, **2017**, 729–734.
39. Vakiloroayaei,A., Shah,N.S., Oeffinger,M. and Bayfield,M.A. (2017) The RNA chaperone La promotes pre-TRNA maturation via indiscriminate binding of both native and misfolded targets. *Nucleic Acids Res.*, **45**, 11341–11355.
40. Janssen,B.D., Diner,E.J. and Hayes,C.S. (2012) Analysis of Aminoacyl- and Peptidyl-tRNAs by Gel Electrophoresis. In: Keiler,K.C. (ed). *Bacterial Regulatory RNA: Methods and Protocols*. Humana Press, Totowa, NJ, pp. 291–309.
41. Duncan,C.D.S. and Mata,J. (2014) The translational landscape of fission-yeast meiosis and sporulation. *Nat. Struct. Mol. Biol.*, **21**, 641–647.
42. Love,M.I., Huber,W. and Anders,S. (2014) Moderated estimation of fold change and dispersion for RNA-seq data with DESeq2. *Genome Biol.*, **15**, 550.
43. Zhong,Y., Karaletsos,T., Drewe,P., Sreedharan,V.T., Kuo,D., Singh,K., Wendel,H.G. and Rätsch,G. (2017) RiboDiff: Detecting changes of mRNA translation efficiency from ribosome footprints. *Bioinformatics*, **33**, 139–141.
44. Bitton,D.A., Schubert,F., Dey,S., Okoniewski,M., Smith,G.C., Khadayate,S., Pancaldi,V., Wood,V. and Bähler,J. (2015) AnGeLi: a tool for the analysis of gene lists from fission yeast. *Front. Genet.*, **6**, 330.
45. Watanabe,Y. and Yamamoto,M. (1994) S. pombe mei2+ encodes an RNA-binding protein essential for premeiotic DNA synthesis and meiosis I, which cooperates with a novel RNA species meiRNA. *Cell*, **78**, 487–498.
46. Yamashita,A., Watanabe,Y., Nukina,N. and Yamamoto,M. (1998) RNA-assisted nuclear transport of the meiotic regulator Mei2p in fission yeast. *Cell*, **95**, 115–123.
47. Knutsen,J.H.J., Rødland,G.E., Bøe,C.A., Håland,T.W., Sunnerhagen,P., Grallert,B. and Boye,E. (2015) Stress-induced inhibition of translation independently of eIF2α phosphorylation. *J. Cell Sci.*, **128**, 4420–4427.
48. Boye,E. and Grallert,B. (2020) eIF2α phosphorylation and the regulation of translation. *Curr. Genet.*, **66**, 293–297.
49. Sanchez,M., Lin,Y., Yang,C.-C., McQuary,P., Campos,A.R., Blanc,P.A. and Wolf,D.A. (2019) Crosstalk between eIF2α and eEF2 phosphorylation pathways optimizes translational arrest in response to oxidative stress. *iScience*, **20**, 466–480.
50. Ohmiya,R., Kato,C., Yamada,H., Aiba,H. and Mizuno,T. (1999) A fission yeast gene (prr1+) that encodes a response regulator implicated in oxidative stress response. *J. Biochem.*, **125**, 1061–1066.
51. Nakamichi,N., Yanada,H., Aiba,H., Aoyama,K., Ohmiya,R. and Mizuno,T. (2003) Characterization of the prr1 response regulator with special reference to sexual development in schizosaccharomyce pombe. *Biosci. Biotechnol. Biochem.*, **67**, 547–555.
52. Calvo,I.A., García,P., Ayté,J. and Hidalgo,E. (2012) The transcription factors Pap1 and Prr1 collaborate to activate antioxidant, but not drug tolerance, genes in response to H2O2. *Nucleic Acids Res.*, **40**, 4816–4824.
53. Cuypers,A., Plusquin,M., Remans,T., Jozefczak,M., Keunen,E., Gielen,H., Opdenakker,K., Nair,A.R., Munters,E., Artois,T.J. *et al.* (2010) Cadmium stress: An oxidative challenge. *Biometals*, **23**, 927–940.
54. Lackner,D.H., Schmidt,M.W., Wu,S., Wolf,D.A. and Bähler,J. (2012) Regulation of transcriptome, translation, and proteome in response to environmental stress in fission yeast. *Genome Biol.*, **13**, R25.
55. Kanoh,J. and Russell,P. (1998) The protein kinase Cdr2, related to Nim1/Cdr1 mitotic inducer, regulates the onset of mitosis in fission yeast. *Mol. Biol. Cell*, **9**, 3321–3334.
56. Millar,J.B., Buck,V. and Wilkinson,M.G. (1995) Pyp1 and Pyp2 PTPases dephosphorylate an osmosensing MAP kinase controlling cell size at division in fission yeast. *Genes Dev.*, **9**, 2117–2130.
57. Shiozaki,K. and Russell,P. (1995) Cell-cycle control linked to extracellular environment by MAP kinase pathway in fission yeast. *Nature*, **378**, 739–743.
58. Degols,G., Shiozaki,K. and Russell,P. (1996) Activation and regulation of the Spc1 stress-activated protein kinase in Schizosaccharomyces pombe. *Mol. Cell. Biol.*, **16**, 2870–2877.
59. Degols,G. and Russell,P. (1997) Discrete roles of the Spc1 kinase and the Atf1 transcription factor in the UV response of Schizosaccharomyces pombe. *Mol. Cell. Biol.*, **17**, 3356–3363.
60. Greenall,A., Hadcroft,A.P., Malakasi,P., Jones,N., Morgan,B.A., Hoffman,C.S. and Whitehall,S.K. (2002) Role of fission yeast Tup1-like repressors and Prr1 transcription factor in response to salt stress. *Mol. Biol. Cell*, **13**, 2977–2989.
61. Guo,L., Ganguly,A., Sun,L., Suo,F., Du,L.-L. and Russell,P. (2016) Global fitness profiling identifies arsenic and cadmium tolerance mechanisms in fission yeast. *G3 (Bethesda)*, **6**, 3317–3333.
62. Hasan,A., Cotobal,C., Duncan,C.D.S., Mata,J. and Copenhaver,G.P. (2014) Systematic analysis of the role of RNA-Binding proteins in the regulation of RNA stability. *PLoS Genet.*, **10**, e1004684.
63. Pelechano,V., Wei,W. and Steinmetz,L.M. (2015) Widespread co-translational RNA decay reveals ribosome dynamics. *Cell*, **161**, 1400–1412.
64. Anda,S., Zach,R. and Grallert,B. (2017) Activation of Gcn2 in response to different stresses. *PLoS One*, **12**, e0182143.
65. Yang,R., Wek,S.A. and Wek,R.C. (2000) Glucose limitation induces GCN4 translation by activation of Gcn2 protein kinase. *Mol. Cell. Biol.*, **20**, 2706–2717.
66. Darnell,A.M., Subramaniam,A.R. and O'Shea,E.K. (2018) Translational control through differential ribosome pausing during amino acid limitation in mammalian cells. *Mol. Cell*, **71**, 229–243.
67. Zaborske,J.M., Narasimhan,J., Jiang,L., Wek,S.A., Dittmar,K.A., Freimoser,F., Pan,T. and Wek,R.C. (2009) Genome-wide analysis of tRNA charging and activation of the eIF2 kinase Gcn2p. *J. Biol. Chem.*, **284**, 25254–25267.
68. Wakasugi,K., Nakano,T. and Morishima,I. (2005) Oxidative stress-responsive intracellular regulation specific for the angiostatic form of human tryptophanyl-tRNA synthetase. *Biochemistry*, **44**, 225–232.
69. Kim,S.J., Yoon,J.S., Shishido,H., Yang,Z., Rooney,L.A.A., Barral,J.M. and Skach,W.R. (2015) Translational tuning optimizes nascent protein folding in cells. *Science*, **348**, 444–448.
70. Stein,K.C., Kriel,A. and Frydman,J. (2019) Nascent polypeptide domain topology and elongation rate direct the cotranslational hierarchy of Hsp70 and TRiC/CCT. *Mol. Cell*, **75**, 1117–1130.

71. Dong,J., Qiu,H., Garcia-Barrio,M., Anderson,J. and Hinnebusch,A.G. (2000) Uncharged tRNA activates GCN2 by displacing the protein kinase moiety from a bipartite tRNA-binding domain. *Mol. Cell*, **6**, 269–279.
72. Wek,S.A., Zhu,S. and Wek,R.C. (1995) The histidyl-tRNA synthetase-related sequence in the eIF2 alpha protein kinase GCN2 interacts with tRNA and is required for activation in response to starvation for different amino acids. *Mol. Cell. Biol.*, **15**, 4497–4506.
73. Zhu,S., Sobolev,A.Y. and Wek,R.C. (1996) Histidyl-tRNA synthetase-related sequences in GCN2 protein kinase regulate in vitro phosphorylation of eIF2. *J. Biol. Chem.*, **271**, 24989–24994.
74. Ishimura,R., Nagy,G., Dotu,I., Chuang,J.H. and Ackerman,S.L. (2016) Activation of GCN2 kinase by ribosome stalling links translation elongation with translation initiation. *Elife*, **5**, e14295.
75. Wu,C.C.C., Peterson,A., Zinshteyn,B., Regot,S. and Green,R. (2020) Ribosome collisions trigger general stress responses to regulate cell fate. *Cell*, **182**, 404–416.
76. Athar,A., Füllgrabe,A., George,N., Iqbal,H., Huerta,L., Ali,A., Snow,C., Fonseca,N.A., Petryszak,R., Papatheodorou,I. *et al.* (2019) ArrayExpress update - from bulk to single-cell expression data. *Nucleic Acids Res.*, **47**, D711–D715.